# Study of Metal-Gate Work-Function Variation using Voronoi cells: comparison of Rayleigh and Gamma distributions

G. Indalecio, A. J. Garcia-Loureiro, N. Seoane and K. Kalna

***Abstract*—We have demonstrated, via validation to experimental data for TiN and Ru, that the grains which appear in the metal gate stacks of nanoscale CMOS devices can be characterized via a two-parameter Gamma distribution ($p$-values $0.17$ and $0.42$ for TiN and Ru). Conversely, a previously presented fit which used Rayleigh distribution does not reproduce the experimental data ($p$-values $3\times10^{-14}$ and $0.0029$ for TiN and Ru). Poisson Voronoi Diagrams (PVDs) are shown as a suitable algorithm to generate grains with Gamma distribution, via fitting of the distribution of 10000 grains. We have also compared the PVD variability against the Rayleigh model. for both TiN and TaN metal gates, and concluded that Rayleigh approach overestimates the device variability (by 11.9% for the TiN and by 7.14% for the TaN).**

***Index Terms*—Characterization, Voronoi diagrams, metal grains, variability, work-function variation**

## I. Introduction

The metal gate granularity (MGG) [1] is one of the most important sources of variability affecting nano-scaled devices studied both experimentally [2] and in simulations [3], [4]. The metal grains that appear in the gate contact will have different sizes and orientations depending on the material and the annealing temperature [5], [6]. The orientation of the metal lattice in each grain will change a work-function (WF) of the metal contact affecting the channel formation and inducing variability into device characteristics [7]. A physically based modelling of the MGG variability requires a realistic characterization of the distribution of the metal grains that accurately reproduces the behaviour found in the experimental devices. Most of the current simulation approaches use square grains which are unrealistic and lack the flexibility to correctly represent gates with very large grains or on the nanoscale regime [8]. Recently, a grain size distribution governed by the Rayleigh distribution was proposed [9] which represented closely simulation results [4]. However, no physical basis has been argued for choosing that particular distribution.

In this paper, we initially establish, via comparison to experimental data, that the random grains arising from the metal gate contacts are characterised via a Gamma distribution. This distribution, unlike the previously adopted Rayleigh fit [9], has a physical justification and will provide a correct description of the metal grain induced device variability. We have demonstrated that our algorithm generates Voronoi cells that follow the expected theoretical Gamma distribution. Finally, we have compared these two distributions, Gamma and Rayleigh, and their predicted MGG variability.

This work is supported by Spanish Government (TIN2013-41129-P, TEC2014-59402-JIN) and EPSRC (EP/I010084/1). Authors thank Dr. Kenji Ohmori for the experimental data provided. G. Indalecio, A. J. García-Loureiro and N. Seoane are with the CITIUS, University of Santiago de Compostela, Spain. E-mail: guillermo.indalecio@usc.es. K. Kalna is with the ESDC, College of Engineering, Swansea University, United Kingdom.

## II. Poisson Voronoi Diagrams

The realistic growth of the metal grains over amorphous substrates is determined by the nature of a deposition process [10]. The first metal atoms that reach the oxide will deposit at random positions and serve as nucleation points. Next deposited atoms will drift towards their closest nucleation points creating a domain with a specific lattice orientation. A Poisson Voronoi Diagram (PVD) [11] reproduces this behaviour being able to generate realistic grains that account for the shape of domains growing from these randomly placed nucleation points. The PVD approach has been previously used [12], [13], [14] to simulate the impact of the metal grain WF variability in nanoscale FinFETs. The physical meaning of the PVD makes it a suitable tool to model the grains of the metal contact. We will demonstrate that the area distribution of the grains generated in a PVD profile is a Gamma distribution. Analysing the area distribution of experimental gates, we are able to validate the Gamma distribution. This process provides the physical basis to use the Gamma distribution that the Rayleigh one lacks.

The PVD is a mathematical structure that consists in seeds of points randomly placed in any $n$-dimensional space. In our case, we are working with a surface that represents a metal gate contact, to generate a profile that can be applied to the device. Once the seeds are located, all the points from the space are classified taking into consideration the nearest seed, defining a PVD. In our case, the domains represent the grains of the metal contact. This profile is generated from material parameters and device dimensions to particularize it for the device under study.

## III. Simulation results

### A. Experimental validation

Both Gamma and Raileigh distributions try to account for the grain distribution of metal gates, so in order to prove which one is more suitable, the best approach is to compare experimental data [2] against Rayleigh and Gamma distributions.

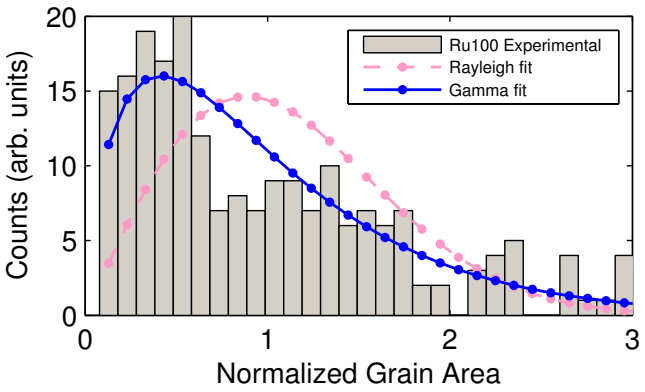


Fig. 1. Experimental distribution of the normalized Ru grain area fitted to Rayleigh and Gamma functions.

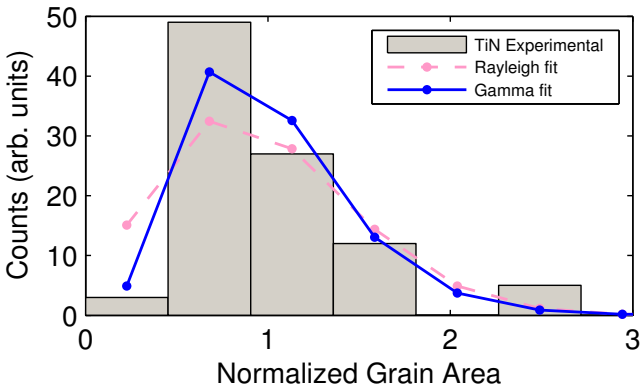


Fig. 2. Experimental distribution of the normalized TiN grain area fitted to Rayleigh and Gamma functions.

To do this comparison, we are going to fit the areas from experimental TEM images to the following density functions:

$$Rayleigh(x;a) = \frac{x}{a^2}\exp\left(-x^2/2a^2\right) \quad (1)$$

$$Gamma(x;a,b) = \frac{1}{b^a\Gamma(a)}x^{(a-1)}\exp\left(-x/b\right)) \quad (2)$$

where $x$ is the normalized grain area and $a$, and $b$ are fitting parameters.

Two metal poly-crystalline films have been compared: TiN, which produces nano-sized grains with mean diameter of 4.3 nm, and Ru, with larger-sized grains with mean diameter of 18 nm [2]. Figs. 1 and 2 show the experimental histograms of the distribution of grain areas (normalised by the mean grain area) for the TiN and Ru metals and their comparison to Rayleigh and Gamma distributions. For both metals, the Gamma distribution accurately reproduces the shape of the experimentally observed metal grains. However, Rayleigh distribution underestimates the number of small grains and overestimates the number of large ones. Using a $\chi^2$ test [15], we can quantify how well these two distributions represent the experimental data. The $\chi^2$ test compares the observed histogram measures ($O_i$) and the expected statistical distribution ($E_i$) using the normalized difference for the $n$ measured points:

$$\chi^2 = \sum_i^n \left(\frac{E_i - O_i}{O_i}\right)^2 \quad (3)$$

Large values of $\chi^2$ represent a mismatch between the observed and the expected data. For any $\chi^2$ exists a corresponding $p$-value (tabulated in standard distribution tables [15]) that represents the probability that the set of data follows the proposed distribution. If the $p$-value is over a lower-bound previously set (typically $0.05$) it is considered that the distribution matches properly the data; if the $p$-value is below the lower-bound the distribution will excessively differ from the observed data.

A $\chi^2$ analysis of the data presented in Figs. 1 and 2 shows that the Gamma distribution of the grain areas for both metals ($p$-values $0.17$ and $0.42$ for TiN and Ru, respectively) fits much better the experimental data than the results produced by Rayleigh distribution ($p$-values $3 \times 10^{-14}$ and $0.0029$ for TiN and Ru, respectively). Therefore, $p$-values show that only Gamma distribution is above the lower-bound of $0.05$, reproducing the experimental data.

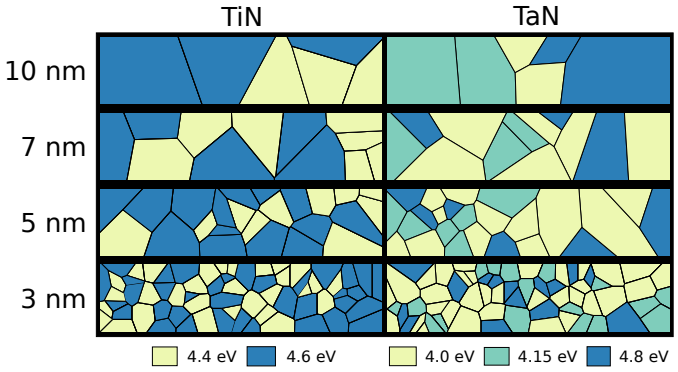


Fig. 3. TiN and TaN gates for different grain sizes. Each colour represent one of the possible WF values for the given material.

### B. PVD simulations: comparison with Rayleigh and Gamma

In this section, we model the distribution of metal grains via Voronoi based simulations. This model will be independent of the metal employed in the gate, since it only depends on the grain distribution and not on the orientation of the grains. As an example, we show TiN and TaN as possible metals for the gate. Their physical properties are collected in Table I. Fig. 3 shows an example of Voronoi WF distributions for these two metal gates for four different grain sizes (10, 7, 5 and 3 nm).

The distribution of grains created via PVD will be now analised to show that Voronoi approach inherently follows the Gamma distribution. We have generated several hundreds of metal grain mappings on the gate with an average grain size of $4.3$ nm. Fig. 4 shows a histogram of the normalized grain area

TABLE I
PHYSICAL PROPERTIES OF THE TIN AND TAN METALS.

| Material | Orientation | Probability | WF (eV) |
|---|---|---|---|
| TiN | $< 200 >$ | 60 % | 4.6 |
| [10] | $< 111 >$ | 40 % | 4.4 |
| TaN | $< 100 >$ | 50 % | 4.0 |
| | $< 200 >$ | 30 % | 4.15 |
| | $< 220 >$ | 20 % | 4.8 |

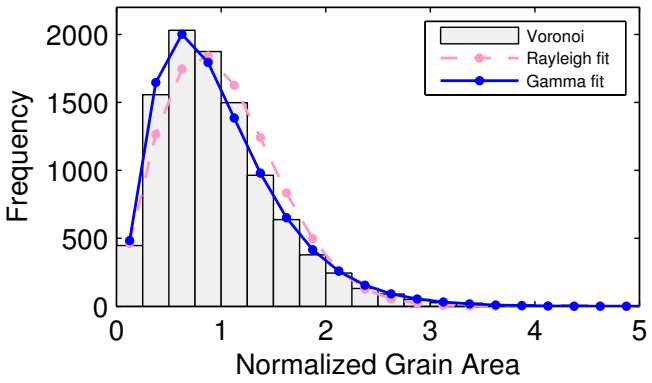


Fig. 4. Distribution of metal grains obtained via Voronoi based simulations. Results have been fitted to both Rayleigh and Gamma distributions.

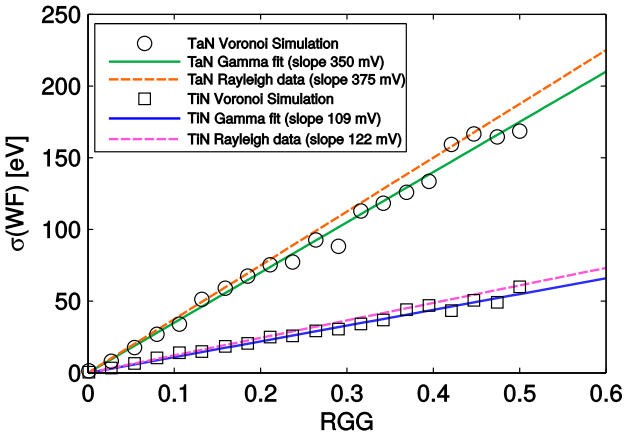


Fig. 5. TiN and TaN gate WF variability Voronoi simulations compared to [4] and to linear Rayleigh and Gamma fits.

distribution for metal grains when Voronoi approach is used together with its fit to Rayleigh and Gamma distributions. The Voronoi distribution fits accurately to a Gamma distribution with a $p$-value of $0.38$. On the other hand, Rayleigh distribution is not only ill-fitted (with a p-value of $0.033$) but it also does not represent correctly a position of the mode of the distribution, which is the grain area that has the largest frequency. This can be seen in Fig. 1, in which modes for both distributions are shifted. Only the Gamma mode matches the experimental data. The Gamma distribution parameters $a$ and $b$ (see Eq. (2)) were fitted to $a$=$b^{-1}$=3.47 via the least squares method. Those values are very close to those predicted by [11] ($a$=$b^{-1}$=3.50). The Rayleigh distribution parameter $a$ fitted to 0.92 is giving the best possible fit to experimental data.

### C. Impact on the estimation of the WF variability

Having demonstrated that the experimental grains follow a Gamma distribution, we aim to analyse the impact of using Rayleigh distribution instead of Gamma distribution to generate the grains for MGG variability studies. To estimate the impact of the gate length and the grain size, we initially define the RGG (average grain size divided by the total gate area) as previously done in Ref. [9]. To obtain an average WF value for all the gates generated via the Voronoi approach, we use the following expression:

$$WF(eV) = \sum_{i=0}^{N} \frac{A_i \cdot WF_i}{A}, \tag{4}$$

where $N$ is the number of grains present in the gate, $A_i$ (nm$^2$) the area of the grain $i$, $A$ (nm$^2$) the total area of the gate, and $WF_i$ (eV) the WF value assigned to the grain $i$. This is a simplification done in order to compare our results with the Rayleigh approach, because it uses an average of grain areas instead of simulating the full device. The downside of this simplification is an underestimation of the variability that will affect all scenarios, as noted in [4].

Fig. 5 shows the TiN and TaN metal gate WF variability extracted from Voronoi based simulations and compares it with: our proposed Gamma fit, and the Rayleigh fit (data extracted from [9]). The number of metal gates which is used to obtain an accurate grain distribution while minimise statistical error depends on the grain size and ranges between $500$ to $1000$.

The Rayleigh linear fit consistently overestimates the gate WF variability with respect to the Gamma fit by 11.9% for the TiN and by 7.14% for the TaN. This overstimation is based on the fact that Rayleigh distribution is unable to correctly capture the grain size distribution, as seen in Figures 1, 2 and 4. This inaccuracy does not play a significant role when the number of grains present in a gate is very large but when there are only a few grains in the gate as in typical nano-scale multi-gate FETs [3], it may lead to a significant overestimation of a variability of the threshold voltage ($V_T$) of devices. As a rough estimation, if we take into account that the $V_T$ of a MOS device depends linearly on its gate WF, the correlation between the metal gate WF and the $V_T$ variabilities [16] is:

$$\sigma(WF)/eV = \sigma(V_T)/mV \tag{5}$$

As an example, the overestimation in $\sigma(V_T)$ is 5 mV when RGG=0.2 if the Rayleigh linear fit is used and it increases to 12.5 mV when RGG=0.5 for TaN.

## IV. Conclusion

We have demonstrated, via validation to experimental data [2], that the metal grains which appear in the metal gate stacks of state-of-the-art nano-scaled devices can be characterized via a two-parameter Gamma distribution. We have shown that a previously presented fit which used Rayleigh distribution [9] is not accurately reproducing the experimental data. However, the two-parameter Gamma distribution of the grain areas is well fitted ($p$-values $0.17$ and $0.42$ for TiN and Ru, respectively) while the Rayleigh distribution of the grains is unsatisfactory ($p$-values $3 \times 10^{-14}$ and $0.0029$ for TiN and Ru, respectively).

Finally, we have compared the Poisson Voronoi Diagram (PVD) variability against the Rayleigh model for both TiN and TaN metal gates. The PVD is an optimum method [17], [18] to generate metal grains since this approach represents the shape

of domains that grow from randomly placed nucleation points as observed in a real fabrication [10], and the grain distribution generated matches the experimental results. We have shown that the Rayleigh approach overestimates the device variability (by 11.9% for the TiN and by 7.14% for the TaN), whereas the variability provided by the Gamma distribution is much closer to the realistic metal gate induced device variability.

## REFERENCES


[1] H. F. Dadgour and K. Banerjee, "Statistical modeling of metal-gate Work-Function Variability in emerging device technologies and implications for circuit design," in *2008 IEEE/ACM International Conference on Computer-Aided Design*. IEEE, nov 2008, pp. 270–277. [Online]. Available: http://ieeexplore.ieee.org/lpdocs/epic03/wrapper.htm?arnumber=4681585

[2] K. Ohmori, T. Matsuki, D. Ishikawa, T. Morooka, T. Aminaka, Y. Sugita, T. Chikyow, K. Shiraishi, Y. Nara, and K. Yamada, "Impact of additional factors in threshold voltage variability of metal/high-k gate stacks and its reduction by controlling crystalline structure and grain size in the metal gates," in *2008 IEEE International Electron Devices Meeting*, no. 110. IEEE, dec 2008, pp. 1–4. [Online]. Available: http://ieeexplore.ieee.org/lpdocs/epic03/wrapper.htm?arnumber=4796707

[3] G. Indalecio, N. Seoane, M. Aldegunde, K. Kalna, and A. J. Garcia-Loureiro, "Variability characterisation of nanoscale Si and InGaAs FinFETs at subthreshold," in *2014 5th European Workshop on CMOS Variability (VARI)*. IEEE, sep 2014, pp. 1–6. [Online]. Available: http://ieeexplore.ieee.org/lpdocs/epic03/wrapper.htm?arnumber=6957085

[4] X. Wang, A. R. Brown, N. Idris, S. Markov, G. Roy, and A. Asenov, "Statistical Threshold-Voltage Variability in Scaled Decananometer Bulk HKMG MOSFETs: A Full-Scale 3-D Simulation Scaling Study," in *IEEE Transactions on Electron Devices*, vol. 58, no. 8. IEEE, aug 2011, pp. 2293–2301. [Online]. Available: http://ieeexplore.ieee.org/lpdocs/epic03/wrapper.htm?arnumber=6131494http://ieeexplore.ieee.org/lpdocs/epic03/wrapper.htm?arnumber=5782949

[5] Q. Zhang, C. Wang, H. Wang, C. Schnabel, D.-g. Park, S. K. Springer, and E. Leobandung, "Experimental Study of Gate-First FinFET Threshold-Voltage Mismatch," *IEEE Transactions on Electron Devices*, vol. 61, no. 2, pp. 643–646, feb 2014. [Online]. Available: http://ieeexplore.ieee.org/lpdocs/epic03/wrapper.htm?arnumber=6704319

[6] S. Deora, G. Bersuker, T. W. Kim, D. H. Kim, C. Hobbs, P. D. Kirsch, K. C. Sahoo, and A. S. Oates, "Positive bias instability in gate-first and gate-last InGaAs channel n-MOSFETs," in *2014 IEEE International Reliability Physics Symposium*. IEEE, jun 2014, pp. 3C.5.1–3C.5.4. [Online]. Available: http://ieeexplore.ieee.org/lpdocs/epic03/wrapper.htm?arnumber=6860625

[7] S. H. Rasouli, K. Endo, J. F. Chen, N. Singh, and K. Banerjee, "Grain-Orientation Induced Quantum Confinement Variation in FinFETs and Multi-Gate Ultra-Thin Body CMOS Devices and Implications for Digital Design," *IEEE Transactions on Electron Devices*, vol. 58, no. 8, pp. 2282–2292, aug 2011. [Online]. Available: http://ieeexplore.ieee.org/lpdocs/epic03/wrapper.htm?arnumber=5934397

[8] Y. Li, H.-W. Cheng, C.-Y. Yiu, and H.-W. Su, "Nanosized metal grains induced electrical characteristic fluctuation in 16-nm-gate high-$\kappa$/metal gate bulk FinFET devices," *Microelectronic Engineering*, vol. 88, no. 7, pp. 1240–1242, jul 2011. [Online]. Available: http://dx.doi.org/10.1016/j.mee.2011.03.037http://linkinghub.elsevier.com/retrieve/pii/S0167931711002966

[9] H. Nam and C. Shin, "Study of High-k/Metal-Gate Work-Function Variation Using Rayleigh Distribution," *IEEE Electron Device Letters*, vol. 34, no. 4, pp. 532–534, apr 2013. [Online]. Available: http://ieeexplore.ieee.org/lpdocs/epic03/wrapper.htm?arnumber=6472749

[10] S. DiCenzo and G. Wertheim, "Monte Carlo calculation of the size distribution of supported clusters," *Physical Review B*, vol. 39, no. 10, pp. 6792–6796, apr 1989. [Online]. Available: http://link.aps.org/doi/10.1103/PhysRevB.39.6792

[11] J.-S. Ferenc and Z. Néda, "On the size distribution of Poisson Voronoi cells," *Physica A: Statistical Mechanics and its Applications*, vol. 385, no. 2, pp. 518–526, nov 2007. [Online]. Available: http://linkinghub.elsevier.com/retrieve/pii/S0378437107007546

[12] G. Indalecio, A. J. Garcia-Loureiro, M. Aldegunde, and K. Kalna, "3D Simulation Study of Work-Function Variability in a 25 nm Metal-Gate FinFET with Curved Geometry using Voronoi Grains," in *Simulation of Semiconductor Processes and Devices (SISPAD), 2012 International Conference on*, 2012, pp. 149–152.

[13] G. Indalecio, N. Seoane, M. Aldegunde, K. Kalna, and A. J. Garcia-Loureiro, "Scaling of metal gate workfunction variability in nanometer SOI-FinFETs," in *2014 15th International Conference on Ultimate Integration on Silicon (ULIS)*, no. Dd. IEEE, apr 2014, pp. 105–108. [Online]. Available: http://ieeexplore.ieee.org/lpdocs/epic03/wrapper.htm?arnumber=6813927

[14] S.-H. Chou, M.-L. Fan, and P. Su, "Investigation and Comparison of Work Function Variation for FinFET and UTB SOI Devices Using a Voronoi Approach," *IEEE Transactions on Electron Devices*, vol. 60, no. 4, pp. 1485–1489, 2013.

[15] P. R. Bevington and D. K. Robinson, *Data Reduction and Error Analysis for the Physical Sciences*, ser. McGraw-Hill Higher Education. McGraw-Hill, 2003. [Online]. Available: https://books.google.co.uk/books?id=JYaZPwAACAAJ

[16] H. F. Dadgour, K. Endo, V. K. De, and K. Banerjee, "Grain-Orientation Induced Work Function Variation in Nanoscale Metal-Gate TransistorsPart II: Implications for Process, Device, and Circuit Design," *IEEE Transactions on Electron Devices*, vol. 57, no. 10, pp. 2515–2525, oct 2010. [Online]. Available: http://ieeexplore.ieee.org/lpdocs/epic03/wrapper.htm?arnumber=5570935

[17] N. Seoane, G. Indalecio, E. Comesana, A. J. Garcia-Loureiro, M. Aldegunde, and K. Kalna, "Three-dimensional simulations of random dopant and metal-gate workfunction variability in an In0.53Ga0.47As GAA MOSFET," *IEEE Electron Device Letters*, vol. 34, no. 2, pp. 205–207, feb 2013. [Online]. Available: http://ieeexplore.ieee.org/lpdocs/epic03/wrapper.htm?arnumber=6407733

[18] G. Indalecio, N. Seoane, M. Aldegunde, K. Kalna, and a. J. García-Loureiro, "Variability Characterisation of Nanoscale Si and InGaAs Fin Field-Effect-Transistors at Subthreshold," *Journal of Low Power Electronics*, vol. 11, no. 2, pp. 256–262, jun 2015. [Online]. Available: http://openurl.ingenta.com/content/xref?genre=article{&}issn=1546-1998{&}volume=11{&}issue=2{&}spage=256